Research Article Vol. 31, No. 13 / 19 Jun 2023 / Optics Express 21399
Optics EXPRESS

# Design of achromatic hybrid metalens with secondary spectrum correction

YANHAO CHU,† XINGJIAN XIAO,† XIN YE, CHEN CHEN, SHINING ZHU, AND TAO LI*

*National Laboratory of Solid State Microstructures, Key Laboratory of Intelligent Optical Sensing and Manipulation, Jiangsu Key Laboratory of Artificial Functional Materials, College of Engineering and Applied Sciences, Nanjing University, Nanjing 210093, China*
†The authors contributed equally to this work.
*taoli@nju.edu.cn

**Abstract:** Metasurface can be used in combination with singlet refractive lens to eliminate chromaticity, in which the metasurface usually works as a dispersion compensator. Such a kind of hybrid lens, however, usually has residual dispersion due to the limit of meta unit library. Here, we demonstrate a design method that considers the refraction element and metasurface together as a whole to achieve large scale achromatic hybrid lens with no residual dispersion. The tradeoff between the meta-unit library and the characteristics of resulting hybrid lenses is also discussed in detail. As a proof of concept, a centimeter scale achromatic hybrid lens is realized, which shows significant advantages over refractive lenses and hybrid lenses designed by previous methods. Our strategy would provide guidance for designing high-performance macroscopic achromatic metalenses.

© 2023 Optica Publishing Group under the terms of the Optica Open Access Publishing Agreement

## 1. Introduction

Optical lens is the core element of imaging systems, which has been developed throughout the history of optical engineering based on refractive optics [1]. Nevertheless, the chromatic aberration coming from the material dispersion severely degrades the imaging quality under white light illuminations. The conventional solution to correct chromatic aberration is to cascade multiple refractive lenses, in which each lens has a different shape and material [1,2]. However, it usually only corrects chromatic aberration at several discrete wavelengths (usually two) in a rigid viewpoint, because one can hardly match the whole dispersion compensation by very limited lens group (two or three). In this case, more pieces of lenses are necessary to access a considerably good achromatism, and thus the whole imaging module needs sacrifice in system complexity, say, large weight and volume, and difficulty in mounting process. The macroscopic size of refractive lenses significantly limits the miniaturization of optical systems. Many efforts have been made to reduce the size and maintain high performance by employing the diffractive optical elements (DOE) [3,4]. However, the Abbe number of DOE is fixed at -3.45, which is hard to be manipulated and usually results in residual chromatic aberrations.

In recent years, metasurfaces, composed of sub-wavelength structures, have attracted increasing interest due to their powerful capability to manipulate optical field [5–9]. Metasurfaces with focusing phase profiles, termed as metalenses, have been studied extensively [7–12]. Towards achromatic metalenses, numerous efforts have already been made both in discrete wavelengths [13–15] and continuous wavelength band [16–19]. Nevertheless, there are fundamental constraint for these "dispersion engineering methods" within very limited meta-units, leading to a size limitation of high-performance achromatic metalens [18,20,21]. The double-layer design can increase the upper limit of size slightly compared with the single-layer design, but the increase on size is limited and it still cannot break through the limitation to achieve large-scale broadband achromatism [22]. To overcome the size limitation, several chromatic aberration meta-correctors

#493216 https://doi.org/10.1364/OE.493216
Journal © 2023 Received 18 Apr 2023; revised 29 May 2023; accepted 30 May 2023; published 9 Jun 2023

Optics EXPRESS

incorporation with refractive elements are implemented [23–27]. However, previous works mainly treated the metasurface as a corrector to compensate the dispersion of the existing refractive lenses with fixed height profile, which will lose a part of design freedom compared with unifying the metasurface and refractive lens in a joint design. Moreover, some of these hybrid lenses exhibited secondary spectrum or higher-order residual dispersion, as is shown in Fig. 1(b), due to the neglect of the group delay dispersion. In order to maximize the design freedom and realize hybrid lenses without residual dispersion, as shown in Fig. 1(c), it is necessary to treat metasurface and refractive lens as a whole, and design the hybrid lenses by analyzing the dispersion comprehensively.

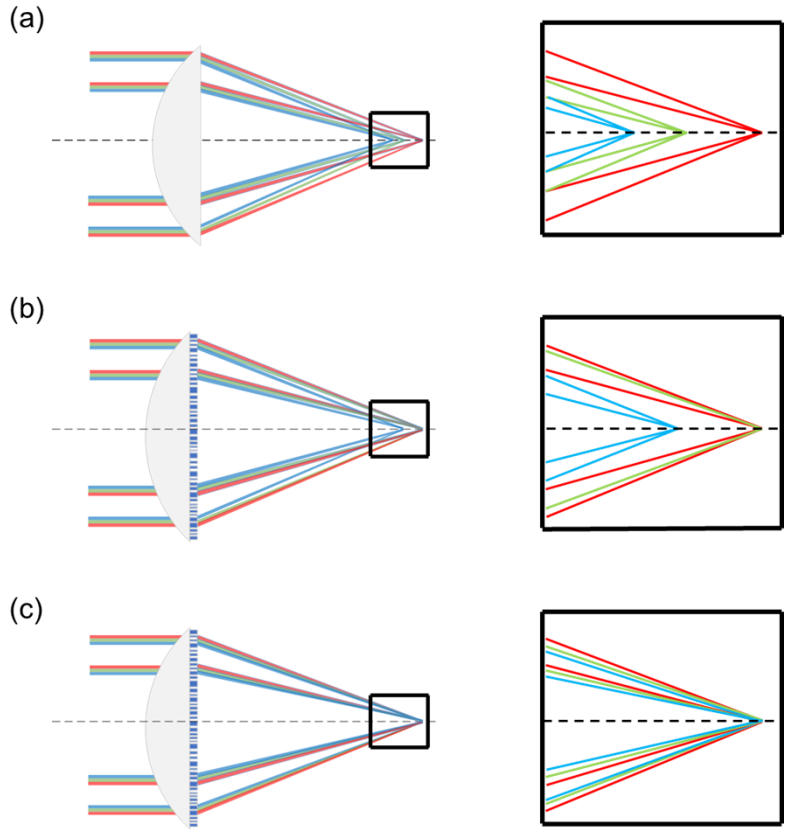


**Fig. 1.** (a) Schematic of refraction lens with chromatic aberration. (b) Schematic of hybrid metalens with residual dispersion. (c) Schematic of hybrid metalens with no residual dispersion.

In this paper, we propose a design to realize achromatic hybrid metalenses with correction of secondary spectrum. By treating hybrid metalenses as a whole, we derive the fundamental restriction relation between the size, numerical aperture (NA) and other parameters of the lenses. Then, a centimeter scale achromatic hybrid metalens is realized. By comparison with common refractive lenses and hybrid lenses designed by previous methods, our design exhibits great advantages in achromatic performance.

Optics EXPRESS

## 2. Results

### 2.1. Design method and fundamental limitations of achromatic hybrid metalenses

The phase profile of a hybrid metalens is composed of three parts - the phase profile $\varphi_R(r, \omega)$ provided by the refractive lens, the propagation phase $\varphi_T(r, \omega)$ and the Pancharatnam-Berry (PB) phase $\varphi_{PB}(r)$ provided by the meta units [23], where $r$ is radial axis and $\omega$ is the angular frequency. Note that the PB phase does not vary with the wavelength that equals to two times the rotation angle of the meta unit [8]. Therefore, the dispersion property of the hybrid metalens is mainly determined by $\varphi_R(r, \omega)$ and $\varphi_T(r, \omega)$, which can both be expanded as a Taylor series with respect to $\omega$ as

$$\varphi_R(r,\omega) = \varphi_R(r) + g_R(r)\omega + \frac{1}{2}G_R(r)\omega^2 + \cdots, \tag{1}$$

$$\varphi_T(r,\omega) = \varphi_T(r) + g_T(r)\omega + \frac{1}{2}G_T(r)\omega^2 + \cdots, \tag{2}$$

where $\varphi_R(r)$ / $\varphi_T(r)$, $g_R(r)$ / $g_T(r)$ and $G_R(r)$ / $G_T(r)$ are the relative phase profile, group delay and group delay dispersion provided by the refractive part and meta unit, respectively. Generally speaking, the whole group delay $g_R + g_T$ determines the difference in the wave packets arrival time at the focus, while the whole higher-order derivative terms (such as group delay dispersion $G_R + G_T$) ensure that the outgoing wave packets are identical [17]. Thus, in order to achieve broadband achromatism, these terms should satisfy relations as follows:

$$\begin{cases} \varphi_T(r) + \varphi_R(r) + \varphi_{PB}(r) = \varphi_{ideal}(r) \\ g_T(r) + g_R(r) = \left.\frac{\partial\varphi_{ideal}}{\partial\omega}\right|_{\omega=0} \\ G_T(r) + G_R(r) = \left.\frac{\partial^2\varphi_{ideal}}{\partial\omega^2}\right|_{\omega=0} \\ \cdots \end{cases}, \tag{3}$$

where $\varphi_{ideal}(r)$, $\partial\varphi_{ideal}/\partial\omega$ and $\partial^2\varphi_{ideal}/\partial\omega^2$ are the relative phase profile, group delay and group delay dispersion of an ideal achromatic lens, respectively. Generally speaking, the phase profile $\varphi_{ideal}(r, \omega)$ provided by an ideal achromatic flat lens follows the hyperbolic relation:

$$\varphi_{ideal}(r,\omega) = -\frac{\omega}{c}\sqrt{r^2 + f^2} + C(\omega), \tag{4}$$

where $f$ is focal length, $c$ is light speed in vacuum and $C(\omega)$ is the spectral degree of freedom. Eq. (1–4) provide a general framework to realize the design of an achromatic hybrid lens. More specifically, we consider the concrete form of $\varphi_R(r, \omega)$, which can be approximately derived based on the accumulation of the optical path [1],

$$\varphi_R(r,\omega) = \frac{\omega}{c}(n(\omega) - n_b)H(r), \tag{5}$$

where $n(\omega)$ is the refractive index of the material of the refractive part, which can be approximately expanded as $n_0 + (dn/d\omega)\,\omega$, $n_b$ is the refractive index of the background and $H(r)$ is the height profile of the refractive part. Put Eq. (4)–(5) into Eq. (3), we can yield

$$\begin{cases} \varphi_T(r) + \varphi_{PB}(r) = C_0 \\ g_T(r) = C_1 - \frac{1}{c}\sqrt{r^2 + f^2} - \frac{1}{c}(n_0 - n_b)H(r) \\ G_T(r) = C_2 - \frac{2}{c}(\frac{dn}{d\omega})H(r) \\ \cdots \end{cases} \tag{6}$$

where $C_0$, $C_1$, $C_2$ are three constants accordingly. Based on Eq. (6), the design method of an achromatic hybrid metalens with fixed diameter and focus length can be constructed following

Optics EXPRESS

three steps. The first is to derive the electric response of all meta units with specific parameters to establish a library through full-wave electromagnetic simulation. Secondly, one should select proper meta units from the meta-unit library and determine the height distribution $H(r)$ based on Eq. (6). Thirdly, we can calculate the PB phase based on Eq. (6) and derive the rotation angle of each meta unit.

Besides, considering that the group delay and group delay dispersion provided by the meta units is finite, there will indeed exist a physical bound on the parameters of achromatic hybrid metalenses. By combining all equations in Eq. (6), a restriction relation can be yielded:

$$R \leq \frac{c \max \Delta\Phi}{\frac{1}{NA} - \sqrt{\frac{1}{NA^2} - 1}} \tag{7}$$

where $R$ is the radius of a hybrid metalens, NA is the numerical aperture, $\Phi$ is the generalized group delay and is defined as

$$\Phi = g_T(r) - \frac{n_0 - n_b}{2dn/d\omega} G_T(r). \tag{8}$$

Here, max $\Delta\Phi$ is the maximum difference of $\Phi$ for all meta units. In fact, Eq. (7) is a generalization of restriction relation for ideal achromatic metalenses [17]. For a single achromatic metalens without refractive part, group delay dispersion $G_T$ needs to be a constant according to Eq. (6), so $\Delta\Phi$ is equal to $\Delta g_T$, which means only $\Delta g_T$ contributes to the size bound according to Eq. (7). While for a hybrid lens, $G_T$ is not necessarily a constant, which means both group delay $\Delta g_T$ and group delay dispersion $\Delta G_T$ contribute to the size bound of achromatic hybrid lenses. Thus, the maximum size of achromatic hybrid lenses is usually much higher than that of achromatic metalenses with fixed meta-unit library.

As a proof of concept, we start by designing an achromatic hybrid lens with relatively small size. The meta-unit library used to construct this lens (denoted as meta-unit library I) is composed of units with five different shapes, as is shown in Fig. 2(a). The application of different shapes of meta-unit aims to provide more adjustable degrees of freedom, enabling the meta-unit library to provide greater dispersion coverage while maintaining a high polarization conversion rate. The material of meta unit is set as $Si_3N_4$. The height of meta units is set as 1200 nm, while the period is set as 400 nm. The geometry parameters of these structures (such as length or width) are designed in the range of 80 to 350 nm. By employing a commercial software (Lumerical FDTD Solutions), we obtained the electrical field responses ranging from 470 nm to 680 nm in this meta-unit library. By setting the material of refractive part as $Si_3N_4$, the distribution of generalized group delay $\Phi$ with respect to $g_T$ can be derived based on Eq. (1) and Eq. (8), which is denoted as group delay space and is shown as blue dots in Fig. 2(b). The pink dashed line denotes the maximum generalized group delay which can be utilized to realize achromatic hybrid lens, which is ~60 fs. As a comparison, the generalized group delay which can be utilized to realize achromatic metalenses is only ~5 fs due to the fact that the group delay dispersion needs to be constant [17], shown as white dotted arrow. Based on Eq. (7), the maximum diameter of the achromatic hybrid metalens with NA fixed at 0.1 can achieve 700 μm for this meta unit library. Due to limited simulation resources, we only select a part of meta units (denoted as orange line) in this case, which correspond to an achromatic hybrid lens with diameter equal to 200 μm and NA equal to 0.1. Then, the height distribution is calculated based on Eq. (6) and schematic diagram of the whole lens is shown in Fig. 2(c).

To characterize the focusing properties of this lens, we calculated focusing intensity distribution in x-z plane for incident light ranging from 470 nm to 680 nm based on scalar diffraction theory [28], and performed full-wave simulations based on Lumerical FDTD Solutions as a validation, as is shown in Fig. 2(d). It is clear that the brightest spots at all wavelengths are almost located at the same position, which demonstrates the achromatism of our design. Besides, the calculated

Optics EXPRESS

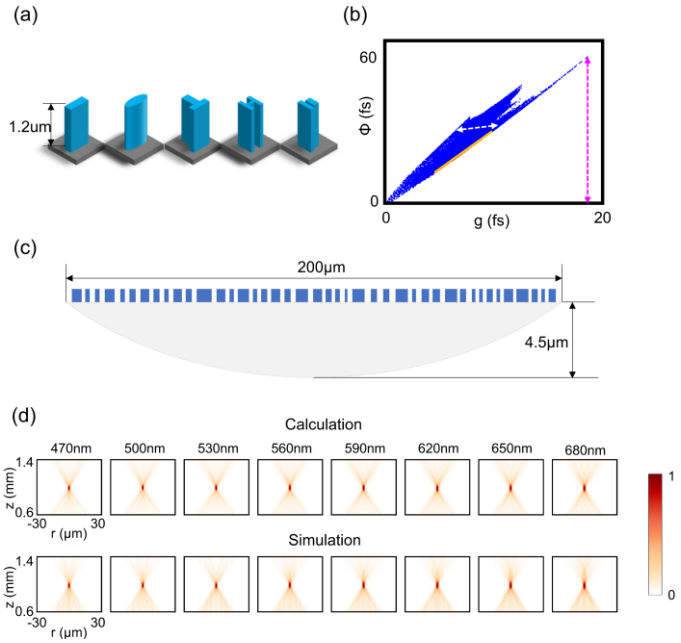


**Fig. 2.** (a) The schematics of five kinds of meta units in library I, where the materials of meta units and refractive part are both set as $Si_3N_4$. (b) The group delay space composed of generalized group delay $\Phi$ and group delay $g$ of meta library I. The pink dashed line and white dashed arrow show the generalized group delay range available for the hybrid lenses and metalenses, respectively. The orange dashed line denotes the chosen meta units to construct the hybrid metalens. (c) Schematic of designed hybrid lens with diameter equal to 200 μm and center thickness equal to 4.5 μm. (d) Calculated and simulated focusing intensity distribution in x-z plane at 8 wavelengths.

results are in good agree with the simulated one. This proves the accuracy of the calculation method. Due to the difficulty of performing full-wave simulation on a large-scale lens (such as centimeter-scale), we will only perform calculation in the next section.

### 2.2. *Centimeter-scale achromatic hybrid metalens*

As is shown above, the maximum diameter of the hybrid lens constructed by meta unit library I is only 700 μm. This is mainly due to two reasons. First, the group delay and group delay dispersion provided by the 1200 nm-height $Si_3N_4$ meta units is relatively small, which can be increased by improving the height and refractive index of the meta units [18]. Second, the refractive index dispersion $dn/d\omega$ is relatively high for $Si_3N_4$ (~0.048 fs), which can be decreased by replacing $Si_3N_4$ with a low dispersion material. Therefore, we constructed meta-unit library II by changing the material of meta unit from $Si_3N_4$ (n~2) to GaN (n~2.4), changing the material of refractive part from $Si_3N_4$ to $SiO_2$ ($dn/d\omega$ ~0.006 fs) and increasing the height of meta units to 2 μm, as is shown in Fig. 3(a). Figure. 3(b) shows the group delay space of the meta-unit library II (blue dots). The maximum generalized group delay reaches 900 fs in this space, which determines the maximum diameter equal to 1.05 cm when NA = 0.1 based on Eq. (7).

By selecting a part of meta units in the meta-unit library II (denoted as orange line in Fig. 3(b)), an achromatic hybrid lens with NA = 0.1 and diameter = 1 cm is realized (denoted as **HLG**). The maximum thickness of refractive part is 500 μm. Then, we calculated focusing intensity distribution in x-z plane for this lens, as is shown in the top row of Fig. 3(c). To illustrate the

Optics EXPRESS

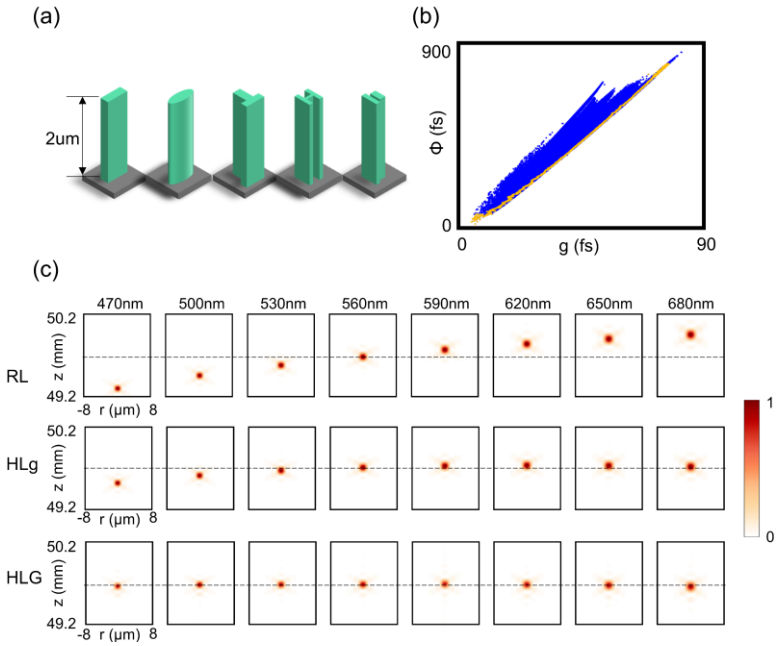


**Fig. 3.** (a) The schematics of five kinds of meta units in library II, where the material of meta units is set as GaN and that of refractive part is set as $SiO_2$. (b) The group delay space composed of generalized group delay $\Phi$ and group delay $g$ of GaN meta units. The orange dashed line denotes the chosen meta units to construct the hybrid lens. (c) Calculated focusing intensity distribution in x-z plane at 8 wavelengths for **HLG** (upper), **HLg** (middle) and **RL** (lower). (d) Focus shift of **HLG**, **HLg** and **RL**. (e) Achromatic Ratio of **HLG**, **HLg** and **RL**. (f) Strehl ratio of **HLG**, **HLg** and **RL**.

necessity of considering both group delay and group delay dispersion, we also design a hybrid lens which only considers group delay (only satisfy the first two equations in Eq. (3), denoted as **HLg**) and a refractive lens (denoted as **RL**) with the same material and parameters. The calculated focusing intensity distribution of these two lenses are exhibited in the middle and bottom rows of Fig. 3(c). The black dashed line in each sub-figure denotes the designed focus length, which shows that **HLG** could focus light in the whole spectrum into almost the same point. However, **HLg** just correct part of chromatic aberrations and there is an obvious deviation at wavelengths shorter than 530 nm.

Figure. 4(a) shows the distribution of the focus shift of three lenses with respect to the wavelength (interval = 1 nm), where the focus shift at 560 nm is fixed at 0 μm for three lenses. To further quantify the achromatic ability of these lenses, we defined the achromatic ratio, which is the ratio of the number of achromatic wavelengths to the number of all the wavelengths in the working spectrum (470 nm-680 nm, interval fixed at 1 nm). The achromatic wavelength here denotes the wavelength at which the absolute value of focus shift is smaller than the depth of focus. Figure. 4(b) shows the achromatic ratio of three lenses, where **HLg** can only correct 70% chromatic aberration (which is consistent with previous report [25]), while **HLG** can correct 100% chromatic aberration. The Strehl ratios of three lenses at designed focus plane are shown in Fig. 4(c). The **HLG** reaches diffraction limit (>0.8) in most area of working spectrum, while Strehl ratios of other two lenses will be relatively low (<0.5) at some wavelengths. The diffraction efficiency of **HLG** is shown in Fig. 4(d). It is calculated by dividing the power in the focal

Optics EXPRESS

spot (the power of transmission light passing through a circular area with radius of $3 \times$FWHM) by the power of co-circularly polarized transmitted light passing through an aperture with the same diameter as the hybrid lens. In the visible bandwidth, the diffraction efficiency of most wavelengths is higher than 80%. All the results above show the advantages and necessity of considering both group delay and group delay dispersion in the design of achromatic hybrid lenses with the correction of secondary spectrum (or residual dispersion).

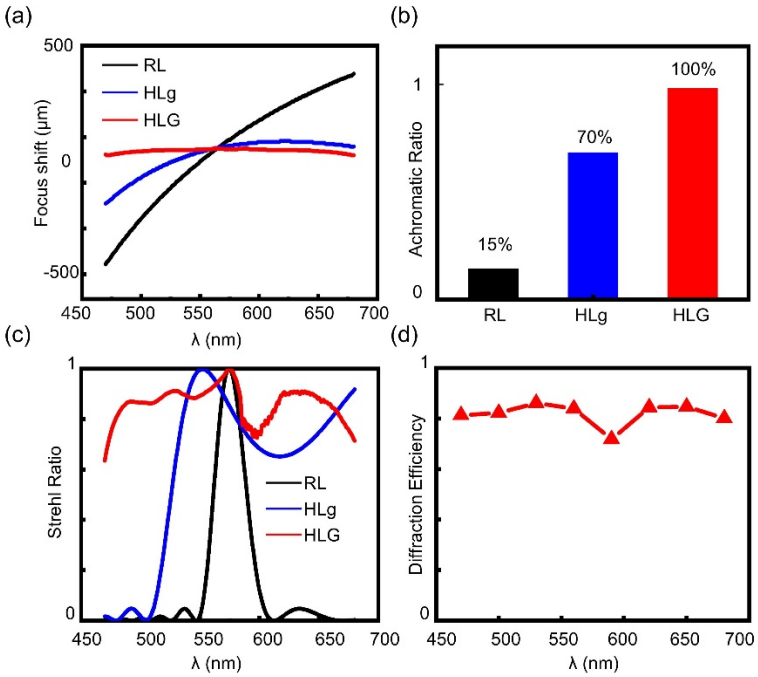


**Fig. 4.** (a) Focus shift of **HLG**, **HLg** and **RL**. (b) Achromatic Ratio of **HLG**, **HLg** and **RL**. (c) Strehl ratio of **HLG**, **HLg** and **RL**. (d) Diffraction efficiency of **HLG**.

## 3. Discussion and conclusion

In this paper, we successfully designed the achromatic hybrid lens with maximum diameter theoretically. However, it should be mentioned that the maximum radius determined by the Eq. (7) can only be achieved by selecting meta units along the edge of the group delay space. In other case, if the height distribution follows a certain shape, the selecting of the meta units will form a line with large curvature in the group delay space, which will add a strong restriction on the size of the hybrid lenses.

In summary, we have proposed a complete design method for achromatic meta-refractive hybrid lens, in which both group delay and group delay dispersion are well engineered to realize achromatism with correction of secondary spectrum. Besides, we derived the upper bound of the size of these kinds of hybrid lenses and pointed out that such bound comes from the finite range of group delay provided by the meta units. The design method provides a new route that possibly promotes the hybrid lenses to real application.

**Funding.** National Key Research and Development Program of China (2022YFA1404301); National Natural Science Foundation of China (12174186, 62288101, 92250304).

**Acknowledgments.** Tao Li thanks the support from Dengfeng Project B of Nanjing University.

**Disclosures.** The authors declare no conflicts of interest.

Optics EXPRESS

**Data availability.** Data underlying the results presented in this paper are not publicly available at this time but may be obtained from the authors upon reasonable request.

## Reference


1. W. J. Smith, *Modern Lens Design.* (McGraw-Hill, 2004).
2. C. G. Wynne, "Secondary spectrum correction with normal glasses," Opt. Commun. **21**(3), 419–424 (1977).
3. N. Davidson, A. A. Friesem, and E. Hasman, "Analytic design of hybrid diffractive–refractive achromats," Appl. Opt. **32**(25), 4770–4774 (1993).
4. T. Stone and N. George, "Hybrid diffractive-refractive lenses and achromats," Appl. Opt. **27**(14), 2960–2971 (1988).
5. N. Yu, P. Genevet, M. A. Kats, F. Aieta, J.-P. Tetienne, F. Capasso, and Z. Gaburro, "Light propagation with phase discontinuities: generalized laws of reflection and refraction," Science **334**(6054), 333–337 (2011).
6. L. Huang, X. Chen, H. Mühlenbernd, G. Li, B. Bai, Q. Tan, G. Jin, T. Zentgraf, S. Zhang, H. Mu, G. Li, and B. Bai, "Dispersionless phase discontinuities for controlling light propagation," Nano Lett. **12**(11), 5750–5755 (2012).
7. H.-H. Hsiao, C. H. Chu, and D. P. Tsai, "Fundamentals and Applications of Metasurfaces," Small Methods **1**(4), 1600064 (2017).
8. M. Khorasaninejad, W. T. Chen, R. C. Devlin, J. Oh, A. Y. Zhu, and F. Capasso, "Metalenses at visible wavelengths: diffraction-limited focusing and subwavelength resolution imaging," Science **352**(6290), 1190–1194 (2016).
9. D. Lin, P. Fan, E. Hasman, and M. L. Brongersma, "Dielectric gradient metasurface optical elements," Science **345**(6194), 298–302 (2014).
10. A. Arbabi, Y. Horie, A. J. Ball, M. Bagheri, and A. Faraon, "Subwavelength-thick lenses with high numerical apertures and large efficiency based on high-contrast transmitarrays," Nat. Commun. **6**(1), 7069 (2015).
11. X. Ye, X. Qian, Y. Chen, R. Yuan, X. Xiao, C. Chen, W. Hu, C. Huang, S. Zhu, and T. Li, "Chip-scale metalens microscope for wide-field and depth-of-field imaging," Adv. Photonics **4**(04), 046006 (2022).
12. C. Chen, X. Ye, J. Sun, Y. Chen, C. Huang, X. Xiao, W. Song, S. Zhu, and T. Li, "Bifacial metasurface enabled pancake metalens by polarized space folding," Optics **9**(12), 1314 (2022).
13. O. Avayu, E. Almeida, Y. Prior, and T. Ellenbogen, "Composite functional metasurfaces for multispectral achromatic optics," Nat. Commun. **8**(1), 14992 (2017).
14. M. Khorasaninejad, F. Aieta, P. Kanhaiya, M. A. Kats, P. Genevet, D. Rousso, and F. Capasso, "Achromatic Metasurface Lens at Telecommunication Wavelengths," Nano Lett. **15**(8), 5358–5362 (2015).
15. H. Li, X. Xiao, B. Fang, S. Gao, Z. Wang, C. Chen, Y. Zhao, S. Zhu, and T. Li, "Bandpass-filter-integrated multiwavelength achromatic metalens," Photonics Res. **9**(7), 1384–1390 (2021).
16. S. Wang, P. C. Wu, V.-C. Su, Y.-C. Lai, M.-K. Chen, H. Y. Kuo, B. H. Chen, Y. H. Chen, T.-T. Huang, J.-H. Wang, R.-M. Lin, C.-H. Kuan, T. Li, Z. Wang, S. Zhu, and D. P. Tsai, "A broadband achromatic metalens in the visible," Nat. Nanotechnol. **13**(3), 227–232 (2018).
17. W. T. Chen, A. Y. Zhu, V. Sanjeev, M. Khorasaninejad, Z. Shi, E. Lee, and F. Capasso, "A broadband achromatic metalens for focusing and imaging in the visible," Nat. Nanotechnol. **13**(3), 220–226 (2018).
18. S. Shrestha, A. C. Overvig, M. Lu, A. Stein, and N. Yu, "Broadband achromatic dielectric metalenses," Light: Sci. Appl. **7**(1), 85 (2018).
19. P. Sun, M. Zhang, F. Dong, L. Feng, and W. Chu, "Broadband achromatic polarization insensitive metalens over 950 nm bandwidth in the visible and near-infrared," Chin. Opt. Lett. **20**(1), 013601 (2022).
20. F. Presutti and F. Monticone, "Focusing on bandwidth: achromatic metalens limits," Optica **7**(6), 624 (2020).
21. X. Xiao, Y. Zhao, X. Ye, C. Chen, X. Lu, Y. Rong, J. Deng, G. Li, S. Zhu, and T. Li, "Large-scale achromatic flat lens by light frequency-domain coherence optimization," Light: Sci. Appl. **11**(1), 323 (2022).
22. Y. L. Wang, Q. B. Fan, and T. Xu, "Design of high efficiency achromatic metalens with large operation bandwidth using bilayer architecture," Opto-Electron. Adv. **4**(1), 200008 (2021).
23. W. T. Chen, A. Y. Zhu, J. Sisler, Y. W. Huang, K. M. A. Yousef, E. Lee, C.-W. Qiu, and F. Capasso, "Broadband Achromatic Metasurface-Refractive Optics," Nano Lett. **18**(12), 7801–7808 (2018).
24. R. Sawant, P. Bhumkar, A. Y. Zhu, P. Ni, F. Capasso, and P. Genevet, "Mitigating chromatic dispersion with hybrid optical metasurfaces," Adv. Mater. **31**(3), 1805555 (2019).
25. R. Sawant, D. Andrén, R. J. Martins, S. Khadir, R. Verre, M. Käll, and P. Genevet, "Aberration-corrected large-scale hybrid metalenses," Optica **8**(11), 1405–1411 (2021).
26. K.-H. Shih and C. K. Renshaw, "Broadband metasurface aberration correctors for hybrid meta/refractive MWIR lenses," Opt. Express **30**(16), 28438–28453 (2022).
27. P. Lin, W. T. Chen, K. M. A. Yousef, J. Marchioni, A. Zhu, F. Capasso, and J. X. Cheng, "Coherent Raman scattering imaging with a near-infrared achromatic metalens," APL Photonics **6**(9), 096107 (2021).
28. J. W. Goodman, *Introduction to Fourier Optics.* (McGraw-Hill, 1968).


218.94.142.34 {ts '2023-12-06 00:15:21'}